Rijksuniversiteit Groningen

Bachelor Thesis

On the Development of a Far-infrared Thermal Image Generator

Author:
Camiel van Hooff

Examiner:
Prof. dr. ir. Caspar van der Wal

Supervisor:
Dr. ir. Gert de Lange

Second Examiner:
Prof. dr. ir. Bart Kooi

A thesis submitted in fulfilment of the requirements for the degree of Bachelor of Science

examined by

Faculteit Wiskunde en Natuurwetenschappen
Rijksuniversiteit Groningen

under supervision of

Instrument Science Group
Netherlands Institute for Space Research

July 2015

"Science is a way of thinking much more than it is a body of knowledge."

Carl Sagan

RIJKSUNIVERSITEIT GRONINGEN

Abstract

Netherlands Institute for Space Research

Bachelor of Science

On the Development of a Far-infrared Thermal Image Generator

by Camiel van Hooff

For the performance characterization of a far-infrared imaging array, a thermal point source image generator is desired. A possible design for this is a square array of resistive heating elements that can be individually controlled. Within this thesis we describe the feasibility of such an image generator. We describe the design, modeling, fabrication and testing of four different 12x12 mm^2 PCBs equipped with 25 SMD thin film resistors of dimensions 1x0.5 mm^2. Measurements with a room temperature thermal camera and an Offner relay system with a cryogenic bolometer operating at 12.5 and 100 μm show good agreement between model and experiment. At room temperature an input power of 1 W results in a rise of 95 $^{\circ}C$, in reasonable agreement with finite element numerical modeling. We do find a discrepancy for the temperature rise of the PCB material, probably because we did not take into account the proper thermal resistance of the PCB to the mounting bracket. The thermal time constant of an individual resistor is in the order of 0.1 s, in agreement with Comsol modeling. By measuring the diffraction limited imaging characteristics around 100 μm, we show that the Airy disk is indeed larger than the resistor dimension, so the resistor indeed can be considered a point source.

Acknowledgements

Special thanks to dr. ir. Gert de Lange, for he helped me beyond my expectations. A surely grounded base of knowledge and wit combined with the natural affection to helping others constantly steered me in the right direction. Working late ment Gert stayed a little longer too, just in case you needed some advise. Also special thanks to prof. dr. ir. Caspar van der Wal and prof. dr. ir. Bart Kooi who gave me the chance to do this research and take some time out of there busy working days to give me feedback on the result. From SRON I want to thank Willem-Jan Vreeling in particular, because he helped me in so many ways at so many aspects, as he does for many other students too. I would like to thank all rest of working staff of SRON as well, for they gave me a very stimulating and pleasant working environment and also were helpful whenever they could. Lastly there is a notable thanks for Inês, Jan, Wim, Valentin and Hallo, who were my fellow students that made me part of a group of friends, but above all made my time at SRON wonderfull.

Contents

Chapter 1

Introduction

SRON, together with ESA, works on a space telescope project called SAFARI. It will house a detector composed of a pixel array. Build to scan a 34 to 210 μm waveband, it aims at far-infrared radiation. To calibrate such a device it is desirable to present it a thermal image of which the characteristics are well known. Some simple idea would be to let a point source move in a plane, hence creating every intensity at any location desired. Unfortunately the extreme sensitivity of SAFARI asks for a low output power at low temperatures of around 5 to 30 K. This induces some problems for mechanical movement. The friction for example will generate to much heat, distorting the image. A possible solution would be electrical movement. An array of resistors, able to control every element individually, can generate a far-infrared image. This thesis will investigate the feasibility of the concept, beginning with characteristics of individual surface mounted resistors. Subsequently the project focuses on the array properties and eventually on the design and production of a thermal image generator.

Chapter 2

Theory

Thermal conduction knows three modes of transport, conduction, convection and radiation. The former two require a material medium. As the project aims at transfer of information through outer space, it being quite empty, the latter is the one best capable of doing just that. The ultimate goal is to design a device that emits an as large as theoretically possible fraction of input power by far-infrared radiation. Combined with doing so on a small surface black body radiation leads to the right direction.

2.1 Radiation of Blackbody and Real Sources

A blackbody is defined by three rules, namely [1];

1. A blackbody absorbs all incident radiation, regardless of wavelength and direction.
2. For a prescribed temperature and wavelength, no surface can emit more energy than a blackbody.
3. Although the radiation emitted by a blackbody is a function of wavelength and temperature, it is independent of direction. That is, the blackbody is a diffuse emitter.

The energy that a blackbody of temperature T emits for a certain wavelength λ in a solid angle Ω is given by Plank's law [2];

$$\frac{P_\lambda}{A}(T) = \frac{2hc^2}{\lambda^5}\frac{1}{e^{\frac{hc}{\lambda kT}} - 1} \tag{2.1}$$

where k is the Boltzmann constant.

The wavelength at which Plank's law has its maximum for a certain blackbody of temperature T is described by Wien's displacement Law [1];

$$\lambda_{max} = \frac{b}{T} \tag{2.2}$$

with b being the constant of Wien. For a wavelength band Plank's law can be integrated over λ and an infinite integral over a hemisphere gives the Stefan-Boltzmann equation[3];

$$\frac{P}{A}(T) = \int_0^\infty I(\nu, T) d\nu \int d\Omega \; j^\star = \sigma T^4 \;, \quad \sigma = \frac{\pi^2 k^4}{60 \hbar^3 c^2} \tag{2.3}$$

where σ is Stefan's constant.

A blackbody has an emissivity ϵ of 1. It is the ratio between real emitted power and Stefan-Boltzmann calculated power. A hand waving argument tells ϵ is high for most mat and dark surfaces, as reflectance is low and absorption is high. On opposite, reflective light materials like polished metals thus have low ϵ.

In the integration of Plank's Law it is assumed radiation is independent of direction. However this is not the case for real bodies and Lambert's law describes the angular dependence of the emissivity by $I(\theta) = I_0 cos(\theta)$.

Radiation does not need a material medium, in fact it does best in vacuum. In most situations, when no (near) vacuum can be realised, electromagnetic waves have to travel trough atmosphere and will be absorbed by it. All molecules in the air absorb at different intensities for certain wavelengths as seen in figure 2.1[4].

2.1.1 Cryogenic temperatures and far-infrared

Safari aims for detecting far infrared radiation between 30 and 210 μm [5]. Table 2.1 shows Wien's displacement law's λ_{max} for a couple of temperatures. All values are calculated with an on-line program called SpectralCalc [4]. It is seen that blackbodies of between 13 K and 96 K all have their λ_{max} in this wavelength range.

2.2 Thermal Conductivity

Creating a localized radiation source requires that one can heat up a small spot, prevent the heat spreading, but also is able to conduct the heat away if wanted. A good understanding of thermal conductivity makes for a to the point design.

FIGURE 2.1: Atmospheric absorption spectrum for 30 to 210 μm.

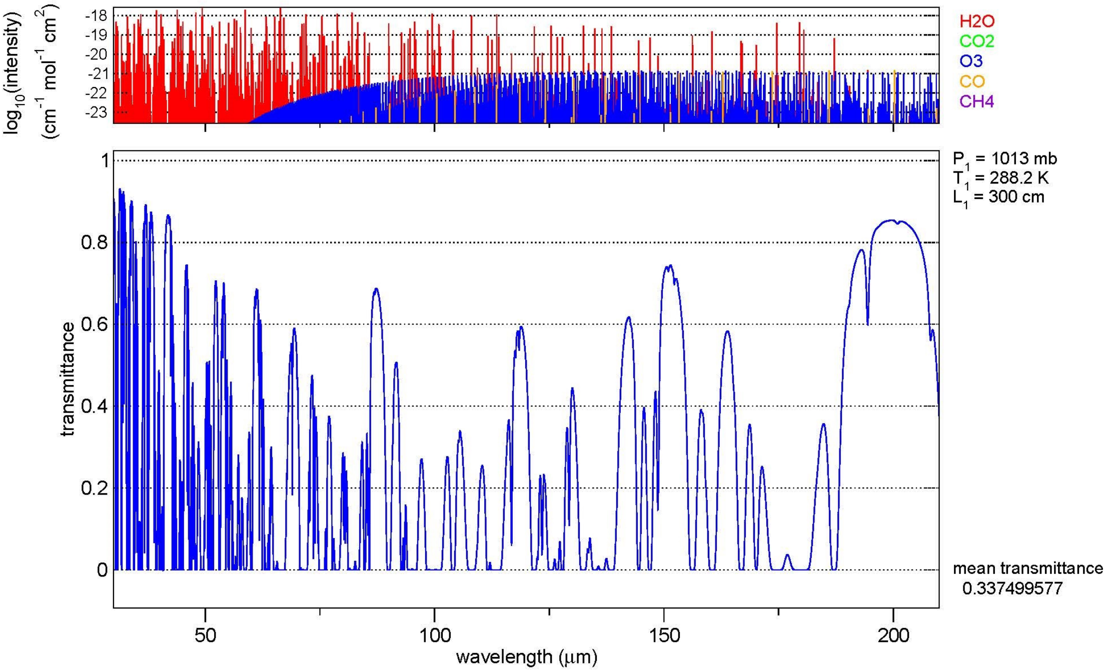

TABLE 2.1: A blackbody at different temperatures with Wien's law λ_{max}, the diameter of its Airy disk given by its ring of first minimum for an optical system with a $f\#$ of 16.7, total emitted power of $1mm^2$ and the percentage of that total power when only integrating over wavelengths larger than respectively $250\mu m$, $100\mu m$ and $12.5\mu m$.

T $[K]$	λ_{max} $[\mu m]$	Airy disk $[mm]$	Total emitted power $[W]$	inf - $250\mu m$ %	inf - $100\mu m$ %	inf - $12.5\mu m$ %
4	724	30	1e-11	100	100	100
13	223	8.5	2e-9	67.1	100	100
40	72.4	2.9	1e-7	8.58	51.9	100
77	37.6	1.5	2e-6	1.60	8.44	99.9
96	30.2	1.2	5e-6	0.877	9.45	99.0
390	7.43	0.40	1e-3	0.0156	0.224	27.5

Fourier's law [6] of thermal conduction

$$q''[W/m^2] = -k\nabla T \tag{2.4}$$

stats heat flux is proportional to the spacial derivative of T by the material's conductivity $k[W/m \cdot K]$. Lets take a plane wall, a common approximation for a one dimensional problem, with distance between the walls x, T_1 at one side and T_2 at the other. Using Fourier's law it turns out temperature distribution is linear dependant on x, i.e. q'' is independent of x.

When heat is generated in a small spot amids other material, it will radially spread out in all directions. For a sphere with T_1 at r_1 and T_2 at r_2 heat rate is given by

$$q[W] = \frac{4\pi k(T_1 - T_2)}{(1/r_1) - (1/r_2)} \tag{2.5}$$

It is constant over r but the area it conducts through is not. If r_1 is much smaller than r_2, heat flux at r therefor is

$$q''(r)[W/m^2] = \frac{k(T_1 - T_2)r_1}{r^2} \tag{2.6}$$

An illustration of this quadratic dependence is given in figure 2.2.

FIGURE 2.2: (a) Heat transfer of a sphere placed in a much larger sphere. Arrows indicating relative size of heat flux and isosurfaces of temperature. (b) Temperature vs radius and gradient of temperature. The gradient decreases quadratic with r.

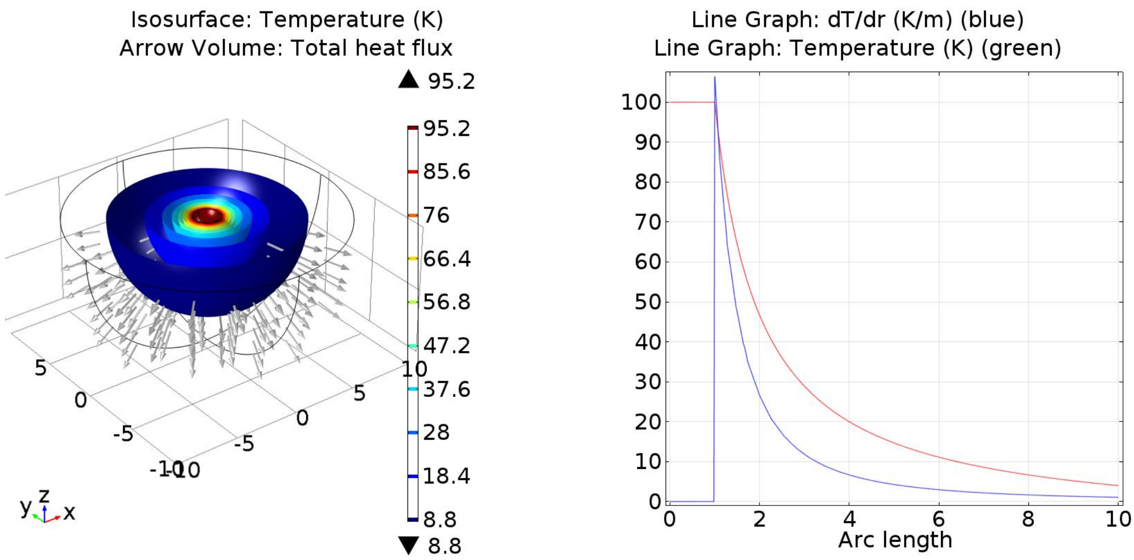

(a) (b)

In all above, thermal conductivity k is assumed to be a constant. In reality k depends on the temperature of the material. At room temperatures, deviation is small, but at cryogenic temperatures k can change orders of magnitude as seen in figure 4.1(a). Because there are many different models concerning k even more equations describe its temperature dependence. For some approximations see section 3.2.

2.3 Optics

There is a lot to say about optics, it could almost be a study on its own. Due to reasons of length of the thesis and time of the research, here follow the most important information and equation. For more information see Optics[7] and the Field Guide to Radiometry[8].

An important characteristic of an optical system is its spacial resolution. It determines the smallest feature it can dissolve. Due to the finite size of the system it will produce an Airy pattern in its imaging plane for every point in its focal plane. The smallest image it can produce, that of a point source, thus is the Airy disk itself. Its diameter, two times the distance from its peak to first minimum, is given as follows;

$$\o Airy = 2.44 \lambda f\# \tag{2.7}$$

Here $f\#$ is the f-number of the optical system given by focal length divided by the aperture diameter. A few øAiry for an optical system with a $f\#$ of 16.7, the same as used in this project's setup, are given in 2.1.

The Rayleigh criterion gives the spatial distance at witch two points are just resolved by a half $\o Airy$. Closer together an optical system can not distinguish two points anymore.

2.4 Infrared Detectors

A simple, fast and easy to use detector is a thermal handheld camera from the company FLIR. It directly shows a thermal image of 240x240 pixels with a refresh rate of 9 Hz. It is best calibrated for -20 to 300 $°C$. For many room temperature measurements it is an easy way to see differences in heat distribution right away. Furthermore it can make movies of the time evolution of the heat spread and can see how a device reacts on a modulated signal.

A much more sensitive radiation strength sensor is a bolometer that is widely used for infrared detection in scientific work. They can measure cryogenic temperatures for they are cooled down to 4 K themselves. Inside is a little piece of material that warms up when radiation hits its surface. The change in resistance is translated to an output voltage that is linearly depending on signal power. Mostly there is a filter in front of the sensor that cuts off all radiation smaller than a given wavelength. This way it does not get overloaded by radiation power of smaller wavelengths in which one mostly is not interested. How much percent of radiation power is left due to the three filters used in this project is given in table 2.1. But that is not all. Given an optical system this also means that it changes the spatial resolution of the system due to a larger Airy disk via equation 2.7.

2.5 Frequency Modulation and Chopping

When measuring radiation from an object that stays constant over time, a sensor like the bolometer produces a lot of noise and drift. Signal processing can filter this noise out of the signal if the part in which you are interested is modulated. When a source is biased with a certain frequency a lock-in amplifier will take out all signal with this specific frequency. What is left over is only signal that is produces by the source. Of coarse the source must be able to do so at reasonable speeds, for otherwise filtering out a modulation would be a patient task and drift would get into the signal anyway. Note bene, the processed signal is not an absolute measurement anymore, but an intensity difference, depending on the modulation depth.

Another way to modulate a signal is not to modulate the source itself, but to place a chopper wheel in front of it. Your detector will measure alternately radiation coming from the chopper wheel and the source. This way a source can be biased continuously. Also here it should be noted that the processed signal is a measure of the difference of signal from the source and the chopping wheel.

Chapter 3

Comsol Model

Comsol Multiphysics is a very effective and easy to use program to model electronics, thermodynamics, mechanics but also radiation. In this project simple models increased the understanding of localised heat sources and so a device model grew up to a final design ready for production.

3.1 One Resistor

In chapter 2 figure 2.2 already showed a greatly simplified model of a device placed on a block of bulk material. Heat flows radially outwards and temperature quickly drops around the source. The source is a hemisphere made of copper and has a large contact area shared with a block of Printed Circuit Board (PCB) material called G10. Surely it needs some geometrical refinement, so the dimensions of a suitable heat source had to be found. To keep the project feasible a surface mounted device (SMD) resistor seemed to be the best solution and its shape was put into the model. The resistor of 0.4 mm long is made of constantan and lies on two copper pads. It is surrounded in vacuum and biased with 0.1 V. The PCB underneath is kept at 4 K at the bottom 15 mm below. A drawing of the resistor and the resulting temperature spread is shown in figure 3.1

Although the spherical symmetry is broken, heat keeps spreading out radially more or less the same as the hemisphere did. That makes it ideal for placement in a square array, for a "pixel" will be able to heat up maximally without heating its neighbour elements too much.

FIGURE 3.1: A SMD resistor with a very simplified Comsol model

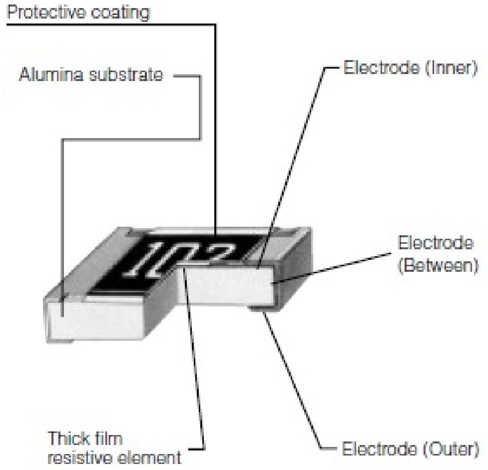

(a) Drawing of a SMD resistor.

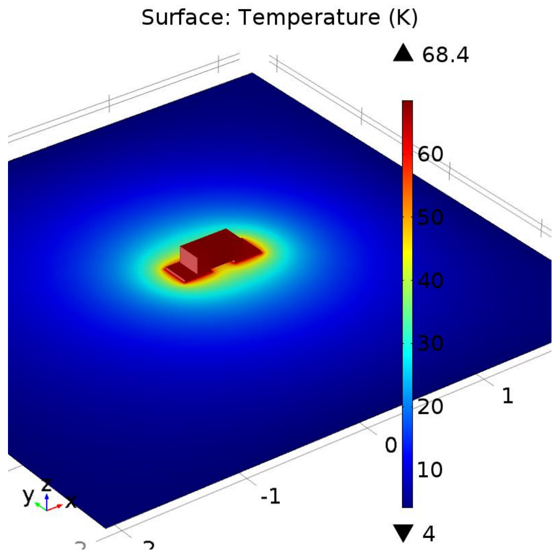

(b) Comsol simulated heat spread.

3.2 Heat Conductivity

With the SMD resistor the three most relevant materials are constantan, copper and G10. Comsol is able to take a function of T as input for k. SAFARI will be tested at cryogenic temperatures, where k changes most strongly. Taking this into the model thus enlarges the reliability. A search through literature and sites listing material properties gave various data [9] [10] [11] [12]. Some functions were fitted and simplified to make sure Comsol will not have a daunting task. The functions are plotted in figure 4.1 (b,c,d) for copper, constantan and PCB material G10 respectively.

3.3 Boundary Conditions

The device will be placed in a near vacuum environment. This directly obviates one problem. The boundary condition at the upside and sides of the model namely are very simple; there is no heat and electrical conduction. For the backside there must be some contact with a bracket, mostly an aluminum block or plate. Since aluminum conducts heat so well and the bracket will be relative large, the backside of the device is cooled so heavily it is assumed to be 4 K for a helium cooled and 77 K a nitrogen cooled cryostat bottom plate. The connection wires for the whole device will be small compared to the bracket, so we will forget about that.

Of coarse the resistors connecting channels, called traces, wont touch the aluminum bracket. The electrical connection from the resistors to the environment will be the

FIGURE 3.2: k vs T for copper, constantan and PCB material.

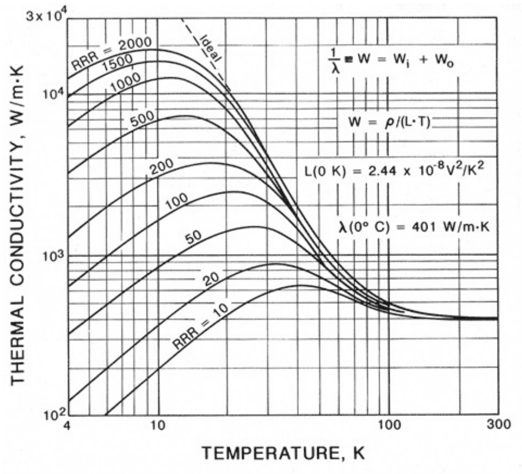

(a) Literature values for copper with different purities.

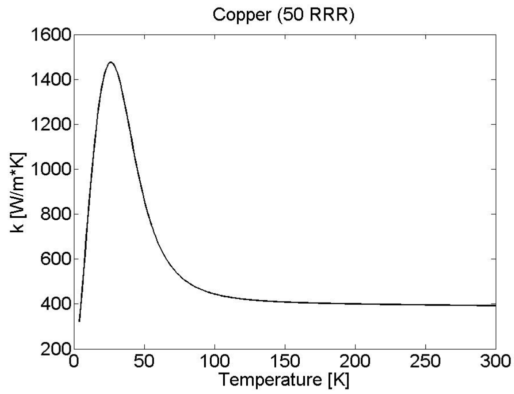

(b) Own approximation of k for copper used for Comsol model.

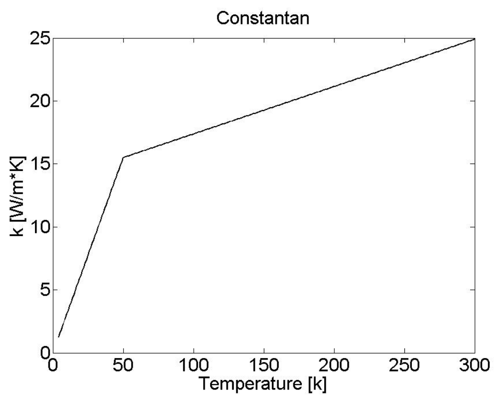

(c) Comsol k for constantan.

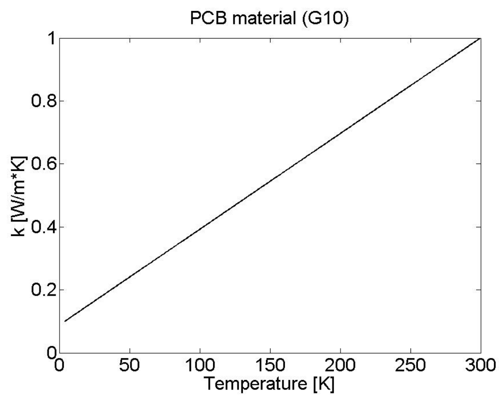

(d) Comsol k for G10.

PCB material and the bias wires. The PCB material is designed to electrically isolate, but because traces and pads will be so close together, lets just take an electrical insulation around the whole device. The bias wires are substitutes by an electrical potential kept at a fixed value.

3.4 Traces, Vias and Planes

3.4.1 Traces

The PCB production process allows for very thin and narrow copper traces. It enhances the thermal isolation of the resistors, for copper conducts so well. It has a k typically 1000 times a large as PCB material (4.1), so even a small copper connection leaks more heat than a much larger base of PCB. Traces are therefore kept as small as possible. Common consumer printing class dimensions are 0.012x0.1 mm^2 in cross section.

3.4.2 Vias

Although small, the traces are the main conductors of heat from the resistors. Trying to make an thermal image in two dimensions, only the upside has to have this thermal characteristics. The third dimension, in the direction of the bracket's thickness, can be used to take the heat from the upside and conduct it to the bracket. A nice thing is that PCBs have the option for vias. They are small holes trough the board who's wall is covered with a thin layer of copper that can be connected with traces if wanted. Its purpose therefore is to make connection from upside and downside traces or even between buried layers of PCBs. But the fact that they are made from copper makes then potentially very effective as heat channels.

From above arises the first idea for a variation in design. If a transistor can be surrounded by many vias, heat will not be able to spread easily through the top plane, because it will be transported downward by the vias instead. A Comsol simulation of the model is shown in is shown in figure 3.3 (a). It is seen that the PCB only warms up much within a ring of vias.

3.4.3 Planes

The upside of trapping the heat as much as possible is that it causes a large temperature gradient. This makes contrast of the pixels high. The downside however is that it impedes cooling down one element. For measurements without a chopper, but with modulation of the input signal, the pixels need to do this quick enough to produces a good signal and to keep measuring times within limits. This induces a trade off between trying to keep the heat in and letting it flow away.

To test whether the speed of the device can be enlarged when a resistor is able to cool down quickly, a copper plane is designed around the resistor. Lying on top of the PCB the plane is shaped around the pads, traces and vias that are directly connected to a resistor. Of course it must not make electrical contact, but it is placed as close by as possible. See figure 3.3 (b) for a Comsol model. Next to the design variations of many vias and a plane, the combination of the two forms the fourth design. Here all vias that are not connected to traces are connected to the copper plane. In this way it must be capable off abduction lots off heat.

FIGURE 3.3: A Comsol model simulation of a PCB design with many vias and a copper plane.

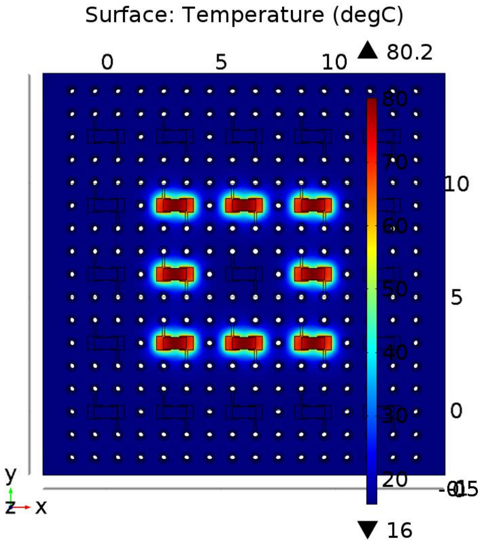

(a) Many vias.

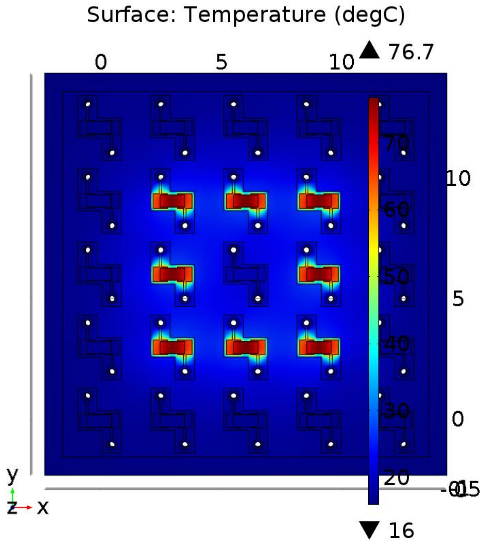

(b) Copper plane.

3.5 Radiation

For very accurate measurements a bolometer, a cooled radiation sensor, is used. It typically needs $10^{-15}W$ input power when measuring a cryogenic source and around $10^{-9}W$ for room temperatures. The optical system with a $f\#$ of 16.7 can redirect 0.1% of the radiation output from source to sensor. This means output power must be at least $10^{-11}W$ at cryogenic and $10^{-5}W$ at room temperatures. Table 2.1 shows some output power values for a 1 mm^2 area of radiating surface. The Comsol simulations in figure 6.4 still produces 100 times too less energy. Enlarging the surface area and the power at which the resistor works resulted in enough power after some tweaking.

3.6 Power

The cryostat used for this experiments is capable of cooling around a few Watts. Biasing the device is limited to a maximum of 200 mA because otherwise the wires in the cryostat warm up too much and can burn trough. Like in our power grid a high voltage makes sure power losses in the bias wires are kept minimal. However working on the project must remain save and so all tests must be executable with no higher voltage than six Volts. All in all this led to the choice of resistors of 15 ω, making for a maximum of 600 mW input power to a single resistor.

3.7 Time Constant

As explained in section 2.5 the warming up and cooling down time is important for signal processing properties. To determine the time constant a resistor on a many via no plane design is biased for somewhat more that 0.1 s. The warming up as also the cooling down is shown in figure 3.4. From the exponential decay the thermal time constant is found to be 0.13 s. A clear warm up and cool down cycle has a duration of about half a second. This should be quick enough for signal processing to get a good signal to noise ratio.

FIGURE 3.4: Comsol simulation of heat build up and cooled down.

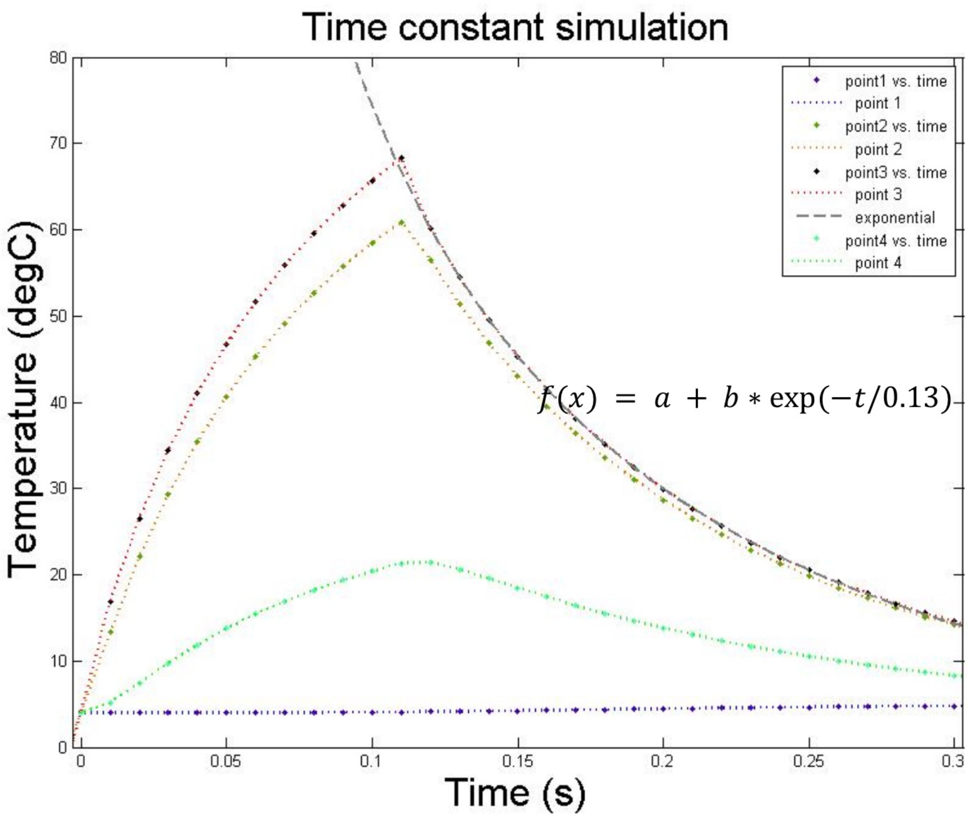

Chapter 4

Production

Out of the books and away from the desk began the hands-on part of the project. Luckily not being born with two left hands, this part naturally appealed to me. All work below is done by myself, sometimes with help of acknowledged people. But before I could get my hands dirty one last step required some extra time in my chair.

4.1 PCB Design and Assembling

Although SRON has its own facilities for PCB printing, my design is made by Eurocircuits. An order is done by sending the layout of all the traces, vias and planes. This is best made in a program like DX Designer. Similarities to programs like AutoCad, Comsol or even Adobe and Office programs are hard to find, so a few days to get acquainted to it were well spent.

To be able to draw a layout an electrical circuit is required. One end of all resistors is connected to one of the pins of a 13-pin header. The other ends are shorted and connected to a single header pin. Exporting this information to the layout part of the program allows for connecting the parts by drawing traces. Luckily the program checks the connections with aid of the electrical circuit. Some patients and TLC resulted in the four layouts of which two are depicted in figure 4.2.

All final dimensions are set to meet the limits of a payable production class clarified in table 4.1.

After receiving the PCB the individual designs where cut to size and went under the microscope. Here the resistors were placed by hand and baked in an oven to melt the solder. Two headers per device completed the boards.

FIGURE 4.1: k vs T for copper, constantan and PCB material.

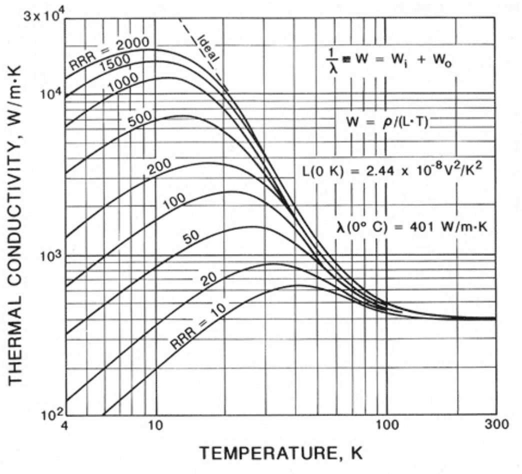

(a) Literature values for copper with different purities.

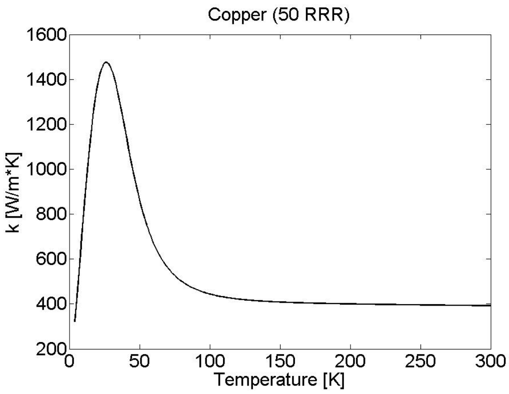

(b) Own approximation of k for copper used for Comsol model.

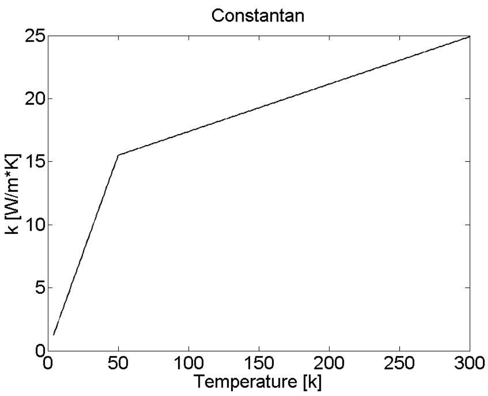

(c) Comsol k for constantan.

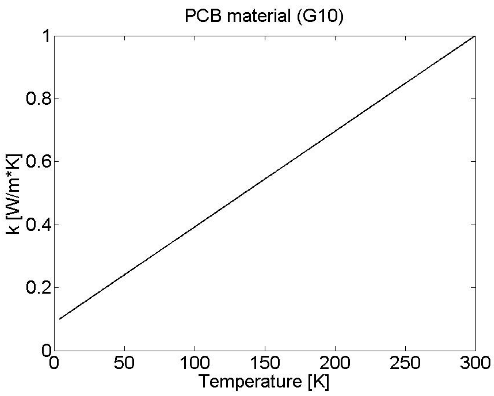

(d) Comsol k for G10.

TABLE 4.1: My caption

Object	Size in mm	Object	Size in mm
Resistor length	1	Pad length	0.6
Resistor width	0.5	Pad width	0.6
Resistor height	0.35	Via outer diameter	0.45
Resistor spacing	3	Via inner diameter	0.25
Copper layer thickness	0.012	Via wall thickness	0.05
PCB thickness	1	Trace width	0.1

To hold the device in place and more importantly, to act as a heat sink, an aluminum bracket was equipped with mounting holes. Finally some cryogenic Kapton tape isolate the back of the vias from the bracket.

FIGURE 4.2: PCB layout of the two designs. The pink lines are the signal traces and the blue ones form the ground. Both are buried in the PCB. The red lines are the signal traces that lie on the top plane and the red square is the copper plane. The large ocher circles are mounting holes.

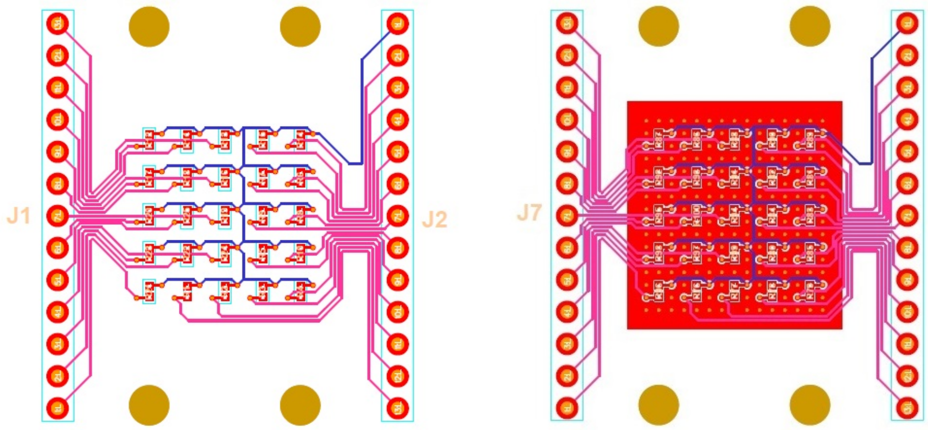

(a) Few vias and no plane. (b) Many vias and with plane.

4.2 Electronics

To individually bias all resistors each pin of the header needs a connection to the outside of the cryostat. Installed on the bottom plate are two 15-pin D-sub connectors wired to the outside via special wires that conduct very little heat. Seemingly all fine a morning soldering gave a headers to D-subs wiring adapter that held 26 connections for the resistors' bias and ground. Later on it turned out the D-sub were connected through for only nine pins. A new adapter used 18 connections to bias the inner array of nine resistors with 3 mm spacing and the "outer" array of nine resistors with 6 mm spacing. This leaves eight resistors on the outer border of the array unconnected.

For use outside the cryostat simple wires with sockets were shorted and can be placed on any pin of the header as desired. With this a single voltage source can bias all resisters wanted.

Chapter 5

Setup

5.1 Offner Relay Re-imaging Optics

In the SAFARI project the detector will consist of an array of sensors. As such a thing is not available for this project, a setup is used to mimic it. A single bolometer is set on an alignment table at one side of an optical system called an Offner re-imaging system. A schematic is shown in figure 5.1[13]. The source, in this case the PCB is placed on the other side of the optical line. This places detector and source at one side of the setup and on the other is a large perfectly spherical concave mirror. It reflects the radiation from the source via a second spherical but convex mirror back to itself and finally to the detector. The second much smaller mirror is in the exact middle of the system. Due to the geometry there is no magnification, hence it is called a re-imaging system. But now comes the great thing, the second mirror is steerable by millidegrees and so steers the beam as shown in 5.1. In this way a scan over a surface or line can be made with only one detector pixel.

5.2 Electronics

The PCB devices are bias by a voltage source capable of producing direct and alternating current with different wave forms. A current source makes sure the voltage source is not power limited. Next to a bias output the voltage has a reference output. It tells a lock-in amplifier at which frequency the bias voltage modulated. When a direct current is used a chopper wheel is placed in front of the PCB device. The lock-in filters out the desired signal and gives an output voltage to a recording computer.

Figure 5.1: Schematic of the Offner re-imaging system.

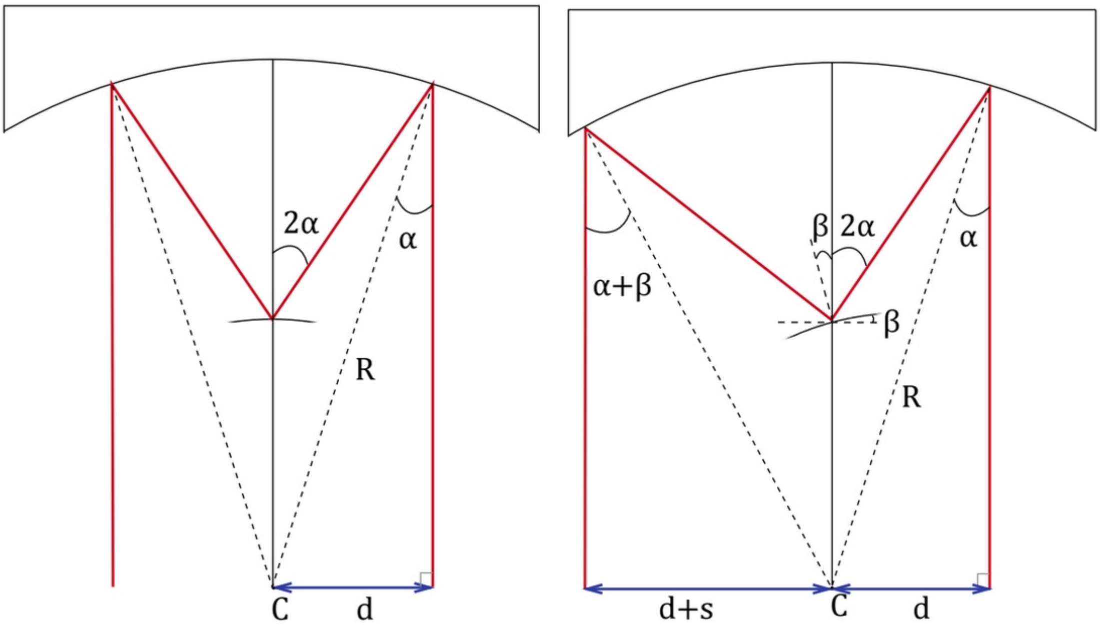

5.3 Golay and XYZ-table

Before testing with the bolometer many testing has been done with a Golay gas cell sensor. It was mounted on a XYZ-table that could be steered in three directions to do a scan over the surface of the source. In between them was an elliptical mirror of which both focal points hold the detector and the source. Unfortunately the sensor turned out to be so much less sensitive as the bolometer, the whole setup was abandoned and the measurements restarted at the Offner setup.

Chapter 6

Measurements

Because measurement at cryogenic temperatures are a lot more difficult and time consuming, the first test are done on room temperature. The FLIR camera is an easy to use detector that quickly gave a good feeling about how the device performed.

6.1 Absolute Temperature

The many simulations in Comsol gave a good overview of expected temperatures. A PCB model with few vias and no copper plane that is biased at 1.3 V at room temperature (25 $°C$) is shown in figure 6.1. The average temperature on top of the resistor is 50 $°C$. If the same PCB model is tested at the same bias it has a total current of 86 mA and a total input power of 1 W. A FLIR camera photo shows a temperature of approximately 43 $°C$ in figure 6.1. The top left one can probably be even higher and thus close to the expectation. This matches all well except for the fact that the PCB material itself warms up more than in the Comsol model.

To see the temperature response of a single resistor it is biased at increasing voltages as seen in figure 6.2. With it comes a fit to a power function that estimates the temperature at 0 V to be 25.3 $°C$, so close to room temperature. The temperature scales almost quadratic with the bias voltage. As input power scales quadratically with voltage increase, a quick reference to equation 2.5 can be made. This said that temperature scales linearly with input power as we consider a simplified double sphere model as in figure 2.2.

Figure 6.1: 8 resistors on PCB with few vias and no plane.

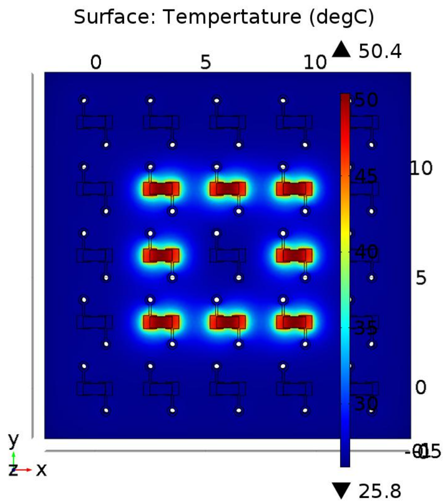

(a) Comsol simulation on a few via and no plane PCB at 1.3V bias.

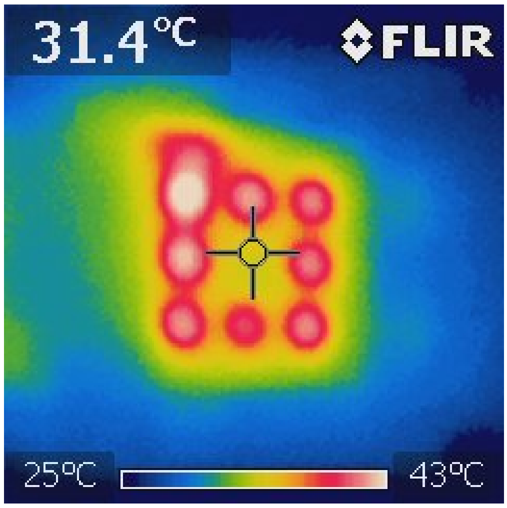

(b) FLIR photo of the same situation.

Figure 6.2: Graph of the maximum temperature on a resistor measured by the FLIR camera versus the bias voltage. Note bene, the bias voltage is not only over the device, but also over the connecting wires.

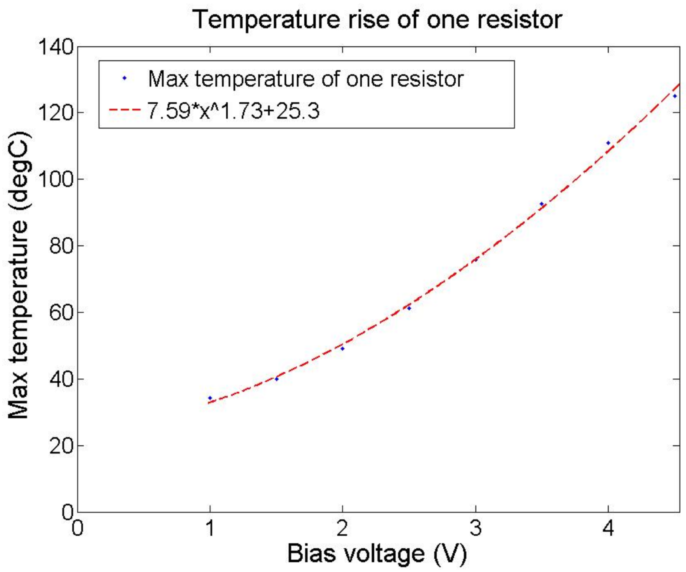

6.2 Temperature Distributions

6.2.1 Copper plane

Although the FLIR camera is handy to roughly measure absolute temperatures, it is even better suited for readily showing temperature distributions. This makes it ideal to look at the differences in the four designs. It turned out the difference in pattern between the few vias and the many vias model were too small to see, but the copper plane gave a clear difference. With that in mind figure 6.3 shows a set of six photos of a many via PCB with(a,b,c) and without(d,e,f) a plane. Of each model three pictures show eight resistors biased with 1.3 V with one resistor spacing, $\sqrt{2}$ resistor spacings and finally two resistor spacings. The eight resistors are placed in a ring so the middle should not be warmed up. In both models the most close packed configuration makes for one large hot spot on the FLIR image. With the $\sqrt{2}$ spacing the design without plane gets a cool yellow spot in the middle and a quite clear hot ring. Last the two spacings test shows that for the copper plane the individual resistors are not clearly distinguishable and has a larger heat spread over the board than the one without.

FIGURE 6.3: FLIR photos of three different resistor distances without a copper layer (a,b,c) and with a copper layer (d,e,f).

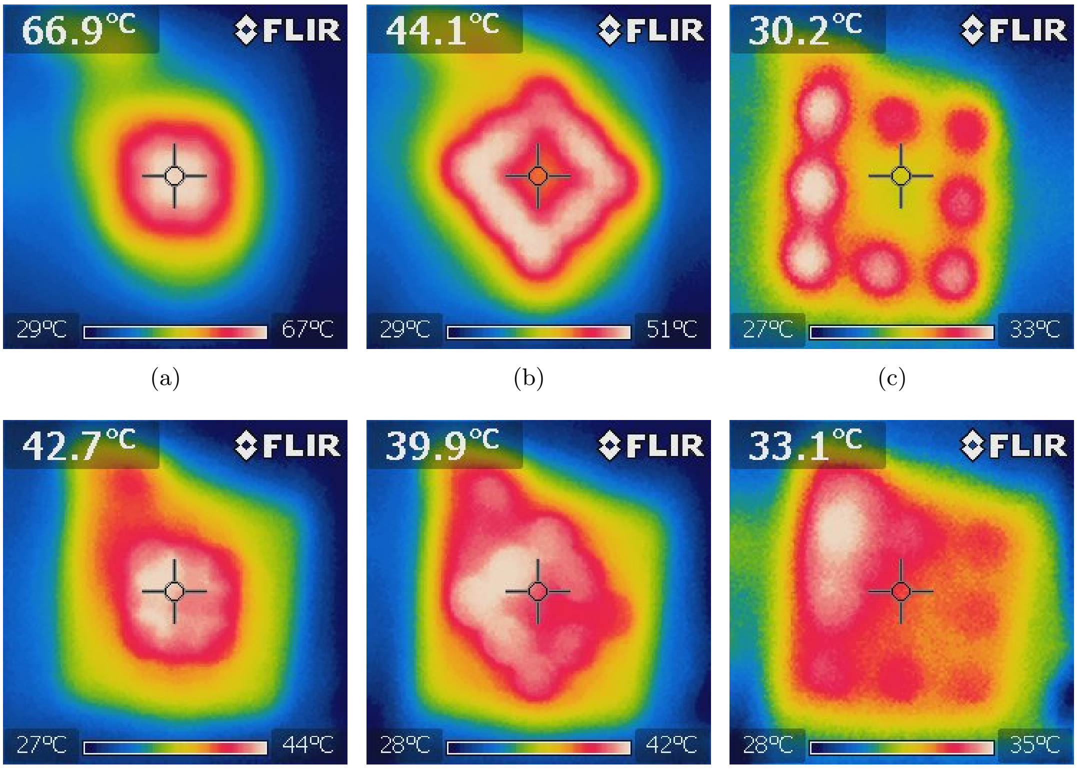

(a) (b) (c)

(d) (e) (f)

6.2.2 Single resistor

When only biasing one resistor the temperature distribution should look like a round spot with a typical dimensions of 2 mm, much alike in figure 3.1. A photo made with the FLIR camera of the PCB with many vias and without a copper plane is shown in 6.4(a). The shape is more or less round and also spans about 2-3 mm. When the same board is imaged with the bolometer a much more refined distribution is observed. Figure 6.4(b) shows a 2d scan with an aperture of 0.3 mm and the filter of 12.5 μm in front. We therefore see a convolution due to only the aperture, because the Airy disk of 51 μm is much smaller than the features. Due to the log scale in z direction a bumped surface can be clearly seen. These actually are the vias. It is possible they are somewhat colder but they also have a lower emissivity and physical holes in them. A comparison between (a) and (b) can only be made off the shape in x and y direction for (a) shows temperature and (b) radiation intensity which goes with σT^4 as in equation 2.3.

FIGURE 6.4: One resistor on the PCB with many vias and no copper plane.

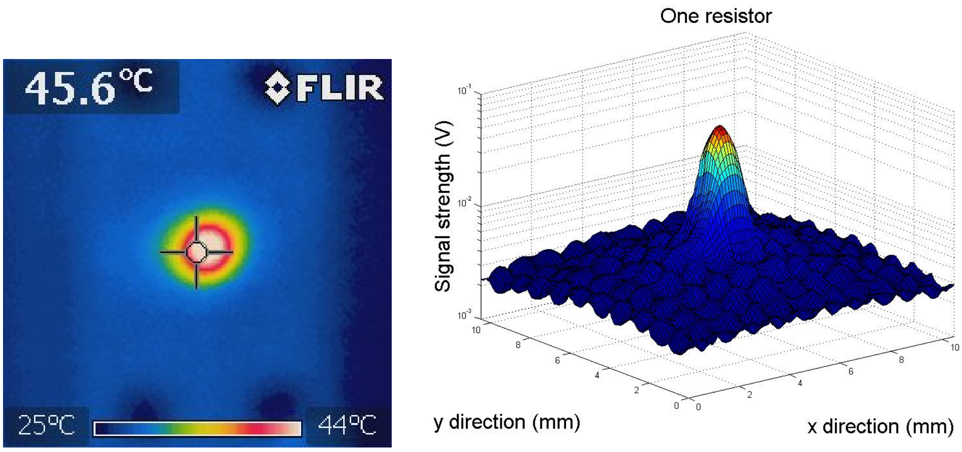

(a) FLIR photo of a single resistor. (b) Bolometer 2D scan of the same resistor.

Many vias

In previous section the FLIR showed the difference due to the copper plane, but could not for the vias. With the bolometer a much more sensitive measurement of the radiation power is done. In the four line graphs of figure 6.5 a comparison is made between the designs with few vias(a) and many vias(b). Both show a broader peak for the copper plane as expected and confirmed above. What is more remarkable is the sharper peak of the few vias design. Simulations of Comsol did not gave that expectation. A possible explanation is that the many vias conduct the heat better to the bracket and cause a lower peak temperature. Therefore the temperature gradient is also lower.

6.2.3 Diffraction limited system

To see whether the device can be used to measure the spatial resolution of a sensor it is important to know whether the pixels can be treated as point sources. In the previous section we clearly saw this was not the case for the cut-off wavelength at 12.5

FIGURE 6.5: Bolometer scan of PCB with few vias and with many vias.

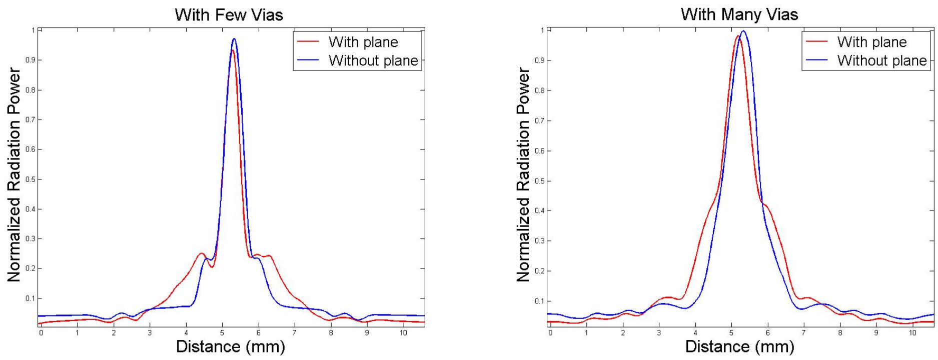

(a) few vias (b) many vias

μm. Setting the filter of the bolometer on the 100 μm position the Airy disk grows to a diameter of at least 4.1 mm. A scan over a single resistor is shown in figure 6.6 as red dots. The test is done in a cryostat of 77 K. Also plotted in the figure is an Airy pattern of 4.1 mm. They totally overlap which implies the resistor can indeed be treated as a point source if only wavelengths of larger than 100 μm are considered.

FIGURE 6.6: Measurement with the 100 μm filter compared with an Airy pattern.

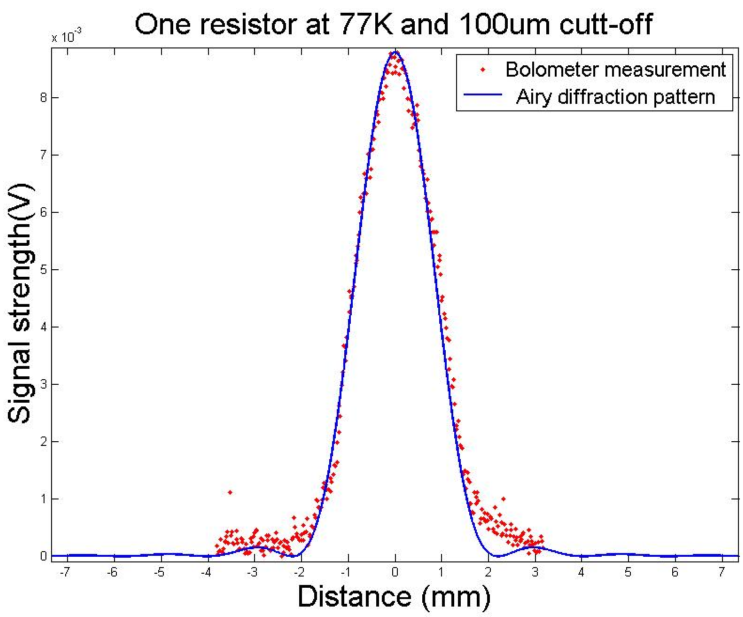

6.2.4 Resistor spaces

To assist the conclusion of the previous section four scans are made. Both filter 12.5 μm and 100 μm are used to do a scan over two resistors that are one resistor spacing apart and two that are two resistor spacings apart. Note the resistor spacing is 3 mm so filter

100 μm should not be able to resolve the two points. Figure 6.7 very well confirms this by showing more or less one peak. Two resistor spacings, so 6 mm, is enough for both wavelength cutt-offs. Note also the broader peaks of the filter 100 μm measurements, due to the Airy disk as discussed in previous section. It should not be forgotten that all graphs are normalized so only shape should be compared.

FIGURE 6.7: Bolometer scan of two resistors with filter 12.5 μm in red and filter 100 μm in blue.

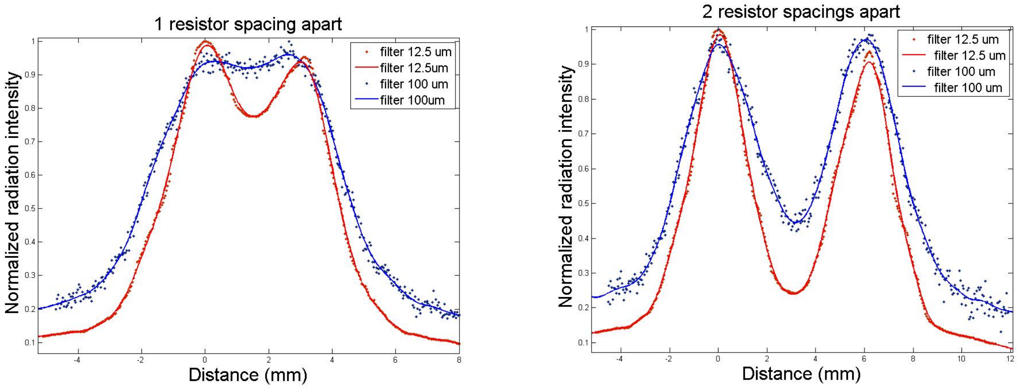

(a) One resistor spacing. (b) Two resistor spacings.

6.3 Time Modulation

As discussed in section 2.5 the time constant of the device is important for implementation in the SAFARI project, for using a chopper wheel is not practical at cryogenic temperatures. The Comsol simulation of section 3.7 predict a time constant of 0.13 s and a rise and fall time of around 2 Hz. To start with the last, videos of a resistor biased at 2 Hz show that the resistor is able to follow the signal nicely. It does not fall back that much as in Comsol but as the PCB stays a lot warmer than expected this is explicable. The resistor almost falls back to that temperature.

Another experiment is done with the bolometer. The lock-in amplifier is coupled not to the frequency of a chopper wheel but to the frequency at which the device is biased. Figure 6.8 shows a log log scale plot of the processed signal strength versus frequency. The bolometer has a wide diaphragm so it looks at the whole board. In red there is the behaviour of a single resistor. For high frequencies it can not follow the bias signal and so there is a low modulation on the radiation output. The lock-in therefore gives a low signal strength. When the frequencies get lower than around 10 Hz the resistors start to follow and the signal increases. The 10 Hz point very well matches with the 0.13 s time constant from Comsol. Furthermore lowering the frequency would eventually cause no drastic increase in signal anymore for it could already follow easily. However if nine wide spaced resistors are biased at around 10 Hz the same increase happens, but at around 0.8 Hz another sharp increase is seen. Here the whole PCB board starts to follow the bias signal and a huge increase in signal strength is the result. The system thus deals with two time constants, one of the resistors and one of the board!

FIGURE 6.8: Measurement of frequency response.

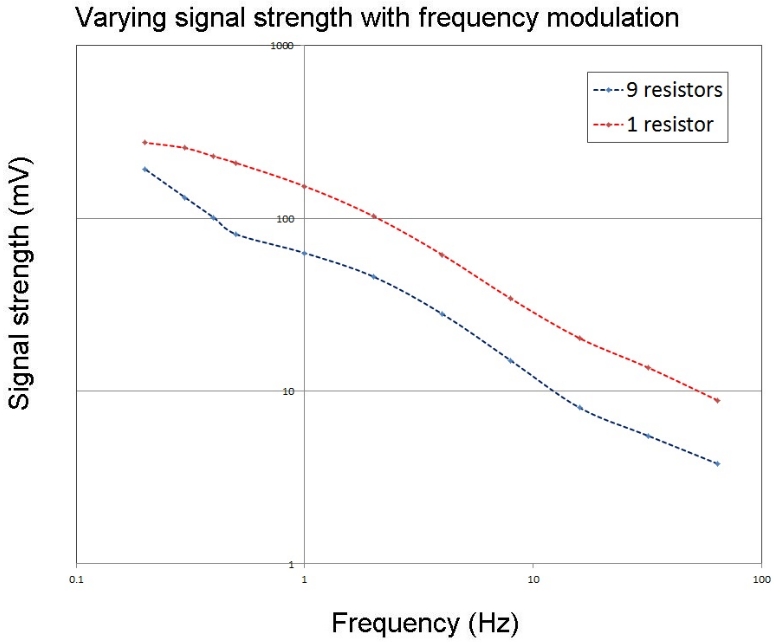

If you think of the device to be two RC-networks in series the graphs can be toughed to be bode plots of the system. For these networks the time constant would be equal to $1/RC$. When the device is scaled down R increases quadratically for it is dependant on surface area, but C drops cubically. Combined this lowers the time constant and smaller devices should thus be quicker. There was no room for experiments on this, but it is a nice toughed altogether. For the same reason the effect of the copper plane on the time constant is regrettably not tested.

Chapter 7

Discussion

7.1 Comsol Comparison

Looking back to the models made in Comsol and the simulations done by it the Comsol model can be said to be a pretty accurate one. An absolute temperature measurement gave a discrepancy of only 5 $^{\circ}C$. This was mainly because the PCB material warmed up more than expected and so the resistors stayed somewhat lower in temperature.

A single resistor causes a heat spot size of the same scale, both between 2-3 mm. Also the shape of the spot was very circular for both cases.

Looking at the copper plane Comsol and measurements confirm a large heat spread over the top plane. The vias on the other hand gave contradicting results. It would be interesting to look at it with greater accuracy.

7.2 Point Source?

Comparison of an Airy pattern with a line scan done with a 100 μm filter showed that from this wavelength and higher the individual resistors can be treated as point sources. Line scans together with Rayleigh's criterion confirmed this. The devices are easily scaled down so point sources for the whole SAFARI range of 30 and 210 μm are in reach.

7.3 Speed

The thermal time constant of the resistors turned out to be small enough for modulation purposes. Here a scale down would cause it to be even lower. A surprising discovery was to find two thermal time constants in the system. A test not ran, but interesting nevertheless would be a frequency response of the copper plane models.

7.4 Best Design and Usefulness

Because of the contradiction between the Comsol model and measurements no favourable position is addressed to either few vias or many vias. A copper plane on the other hand causes such large heat spots that they are not advisable.

All in all the devices showed that they would make for a good thermal emitter to test characteristics of SAFARI if they are scaled down, which is easily possible.

Bibliography

[1] F. P. Incropera, D. P. Dewitt, T. L. Bergman, and A. S. Lavine. Fundamentals of heat and mass transfer. pages 736–739, 2007.

[2] Infrared Training Institute. Black body information. 2012. URL http://www.infraredtraininginstitute.com/black-body-radiation/.

[3] Wikipedia.org. Black body radiation. 2015. URL https://en.wikipedia.org/wiki/Black-body_radiation.

[4] Inc GATS. Atmospheric paths. 2015. URL http://www.spectralcalc.com/atmospheric_paths/paths.php.

[5] F. P. Helmich. Spica/safari. 2015. URL https://www.sron.nl/spica--safari-lea-menu-2661.

[6] F. P. Incropera, D. P. Dewitt, T. L. Bergman, and A. S. Lavine. Fundamentals of heat and mass transfer. page 59, 2007.

[7] E. Hecht. Optics fourth edition. pages 443–485, 2002.

[8] B. G. Grant. Field guide to radiometry. pages 5,17, 1957.

[9] Copper Development Association Inc. 2015. URL http://www.copper.org/resources/properties/cryogenic/.

[10] S. W. Van Sciver. Helium cryogenics. page 35, 2012.

[11] CERN Accelerator scool. 2013. URL http://indico.cern.ch/event/194284/contribution/7/material/4/0.pdf.

[12] A. L. Woodcraft and A. Gray. A low temperature thermal conductivity database. pages 2–3, 2009.

[13] E. Schallig. A far-infrared beam-steering offner relay for safari. page 24, 2015.